Ultra-Wide Bandwidth (UWB) Signal Propagation for Outdoor Wireless Communications

Moe Z. Win, Fernando Ramírez-Mireles, and Robert A. Scholtz
Communication Sciences Institute
Department of Electrical Engineering-Systems
University of Southern California, Los Angeles, CA 90089-2565 USA

Mark A. Barnes
Time Domain Systems, Inc.
6700 Odyssey Drive, Suite 100, Huntsville, AL 35806 USA

ABSTRACT— **Ultra-wide bandwidth (UWB) signal propagation experiment is performed in a rural terrain to characterize the outdoor UWB signal propagation channel. The bandwidth of the signal used in this experiment is in excess of one GHz. The test apparatus and measurement technique are described. From the measured pulse response the mean delay, delay spread, propagation loss and forestation loss are determined.**

I. INTRODUCTION

Propagation environments place the fundamental limitations on the performance of the wireless communications systems. An accurate characterization of the propagation channel is crucial in many aspects of communication systems engineering such as deriving optimal methods, estimating the system performance, performing design trade-offs, etc. Many propagation measurements have been made over the years on both indoor and outdoor channels with much "narrower bandwidths" with emphasis on urban and man-made environments. However, characterization of UWB signal propagation channel in a rural terrain has not been available previously in the literature. Previous measurements and models are inadequate for applications that require communications mainly in natural terrain with very little man made objects. This paper describes a test apparatus and technique of a pilot experiment to characterize UWB communication channel through a forest.

II. EXPERIMENTAL DESIGN

A. Measurement System.

The measurement system for obtaining the impulse response is shown in figure 1. The test apparatus consists of a periodic pulse generator that transmits UWB radar-like pulses, with bandwidth on the order of 1.3 GHz, at every 500 nanoseconds using a step recovery diode-based pulser connected to a UWB antenna. A probe antenna was placed near the transmitter's antenna and a fixed length of cable was routed to the receiver for triggering. Therefore all recorded multipath profiles have the same absolute delay reference, and time delay measurements of the signals arriving to the receiver antenna via different propagation paths can be made. The receiver is set in such a way that every 50 nanoseconds window of measurements contains 1024 samples throughout the experiments. This implies that the time resolution is 48.828 picoseconds between the samples and the equivalent sampling rate is 20.48 GHz.

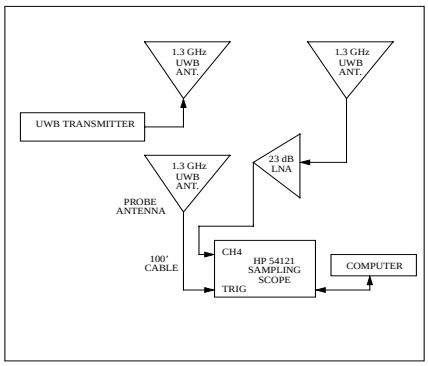

Fig. 1. Block Diagram showing the test apparatus configuration.

The research described in this paper was supported in part by the Joint Services Electronics Program under contract F49620-94-0022, and in part by the Integrated Media Systems Center, a National Science Foundation Engineering Research Center with additional support from the Annenberg Center for Communication at the University of Southern California and the California Trade and Commerce Agency.

The graduate studies of Mr. Ramírez are supported by the Conacyt Grant.

The corresponding author can be reached by E-mail at win@milly.usc.edu

B. Measurement Environment

The test area is typical of the dense native upper Alabama forest, consisting of southern pines, oaks, dogwoods, cedars, sugar maples, thickets and poison ivy. The multipath propagation channel is frozen during the measurement time by making sure that people in the vicinity of the transmitter and receiving antennas have stopped moving.

C. Experimental Procedure

A short duration pulse is transmitted as an excitation signal of the propagation channel. The received signal represents the convolution with the excitation pulse and impulse response of the channel. Time varying characteristic of the channel can be observed by periodic repetition of the pulse transmission. A pulse repetition time of this pulse equal to 500 ns is sufficiently short to characterize the time varying nature of the individual propagation pulse, and long enough to ensure that multipath response of the previous pulse transmission has decayed. Using the average capability of the receiver apparatus, 32 sequentially measured multipath profiles at these same exact location are averaged to reduce noise levels. During each of the multipath profile measurements, both the transmitter and receiver are kept stationary. The measurements are made at c feet away from the transmitter and d feet deep into the line of foliage. Figure 2(a) shows the 200 nanoseconds long typical multipath measurement where the receiver located at (c,d) = (10,0) feet. Similar results for (c,d) = (30,20) and (c,d) = (50,40) are shown in figure 2(b) and 2(c), respectively. The received signal is matched-filtered to produce the corresponding power-delay profiles shown at the bottom of in figures 2(a), 2(b) and 2(c).

III. MULTIPATH PROFILE PARAMETERS

The baseband transmitted pulse is $p(t)$. The channel is represented by multiple paths having real positive gains $\{\beta_k\}$ and propagation delays $\{\tau_k\}$, where k is the path index. Thus, the channel impulse response is given by

$$h(t) = \sum_k \beta_k \delta(t - \tau_k),$$

where $\delta(\cdot)$ is the Dirac delta function.

The received signal is the time convolution of $p(t)$ and $h(t)$ and is given by

$$x(t) = \sum_k \beta_k p(t - \tau_k).$$

This signal is matched-filtered to improve the signal to noise ratio. The filtered signal is given by

$$y(t) = \sum_k \beta_k \gamma(t - \tau_k),$$

where $\gamma(t)$ is the convolution of $p(t)$ with $p(-t)$.

In this experiment we assume that there is no overlap of pulses, i.e., $|\tau_k - \tau_l| > 2$ nanoseconds when $k \neq l$. Hence, after passing through a square envelope detector, the power profile is

$$s(t) \stackrel{\triangle}{=} |y(t)|^2 = \sum_k \beta_k^2 |\gamma(t - \tau_k)|^2.$$

Figure 2 shows three examples of $x(t)$, $y(t)$ and $s(t)$.

A. RMS Delay Spread and Mean Excess Delay

Two simple parameters that are useful in describing the overall characteristics of the multipath profile $h^2(t)$ are the rms delay spread

$$\sigma_\tau \stackrel{\triangle}{=} \sqrt{\overline{\tau^2} - (\overline{\tau})^2}$$

where

$$\overline{\tau^n} \stackrel{\triangle}{=} \frac{\sum_k \tau_k^n \beta_k^2}{\sum_k \beta_k^2}; \qquad n = 1, 2,$$

and the mean excess delay $\overline{\tau}$. The above parameters can be obtained directly from the received power profile $s(t)$ [Saleh, 1987][Hashemi, 1993]. Define the received power profile moments

$$M_n = \sum_k (t_k - T_A)^n s(t_k); \qquad n = 0, 1, 2,$$

and the transmitted pulse moments

$$m_n = \sum_k (t_k - T_B)^n \gamma^2(t_k); \qquad n = 0, 1, 2,$$

where T_A and T_B are the times where $s(t)$ and $\gamma(t)$ start taking values different from zero, respectively. Also define the corresponding averages

$$\overline{t_s^n} = \frac{M_n}{M_0}; \qquad n = 1, 2,$$

$$\overline{t_\gamma^n} = \frac{m_n}{m_0}; \qquad n = 1, 2,$$

and the variances

$$\sigma_s^2 = \overline{t_s^2} - \overline{t_s}^2,$$

$$\sigma_\gamma^2 = \overline{t_\gamma^2} - \overline{t_\gamma}^2.$$

It can be shown that

$$\overline{\tau} = \overline{t_s} - \overline{t_\gamma},$$

and

$$\sigma_\tau = \sqrt{\sigma_s^2 - \sigma_\gamma^2}.$$

The experimental values for $\overline{\tau}$ and σ_τ are shown in table I. It can be seen that $\overline{\tau}$ and σ_τ increases as a function of distance, except the last measurement.

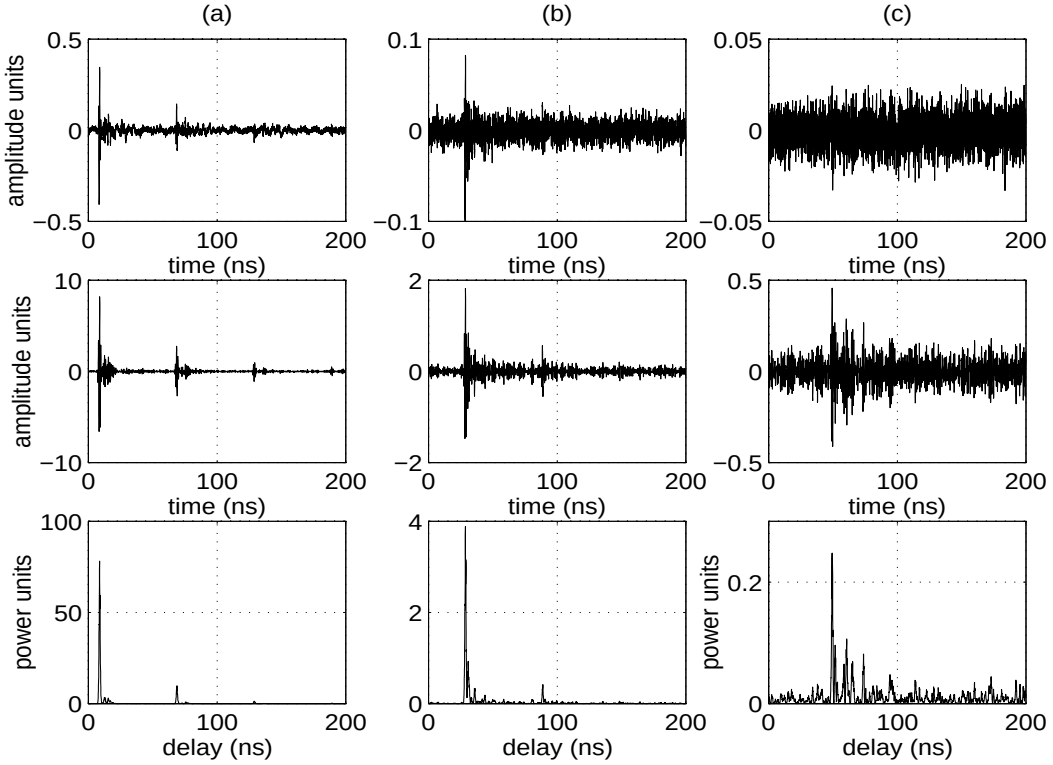

Fig. 2. Propagation losses through foliage and trees. Signal received at distance c feet from the transmitter and d feet depth into the line of foliage. (a) c=10, d=0. (b) c=30, d=20. (c) c=50, d=40. Top: Received signal $x(t)$. Middle: Matched-filtered signal $y(t)$. Bottom : Power-delay profile $s(t)$.

range (m)	forest depth (m)	Exp. Value τ (ns)	Exp. Value σ_τ (ns)
3	0	13.77	31.02
6.1	3	15.21	32.72
9.1	6.1	22.49	38.08
12.2	9.1	33.52	43.09
15.2	12.2	63.55	48.98
18.3	15.2	34.26	34.26

TABLE I

ESTIMATED VALUES OF $\overline{\tau}$ AND σ_{tau} AS A FUNCTION OF RANGE.

B. Power Attenuation

Another simple parameter that is useful in describing the characteristics of the multipath profile $s(t)$ is the total multipath power gain

$$G \stackrel{\triangle}{=} \sum_k \beta_k^2 < 1$$

G can be calculated from the profile moments as follows

$$G = \frac{M_0}{m_0}$$

The spatial average of the power gain G_{av} as a function of the distance r from the transmitter is, in general, a decreasing function of r. The logarithmic value of this attenuation is

$$L(r) = -10log_{10}\left[\frac{G_{av}(r)}{G_{av}(r_0)}\right]$$

where r_0 is a reference point. $L(r)$ can be calculated from the profile moments as follows

$$L(r) = -10log_{10}\left[\frac{M_0(r)}{M_0(r_0)}\right]$$

The plot of $L(r)$ is shown in figure 2, along with the free-space propagation loss

$$L_\alpha(r) = -10log_{10}(r^{-\alpha})$$

for $\alpha = 2$ and $\alpha = 3$.

C. Forestation Losses

We are also interested in evaluating the so called peak "forestation losses" due to foliage and trees. In particular, we want to confirm that a particular narrowband loss model can be applied to our ultra-wide band case. The narrowband model is [Weissoerger, 1982]

$$L_f = \begin{cases} 0.45f^{0.284}d_f & ; 0 \le d_f \le 14m, \\ & \quad f \ge 0.2GHz \\ 1.33f^{0.284}d_f^{0.588} & ; 14m \le d_f \le 400m, \\ & \quad f \ge 0.2GHz \end{cases}$$

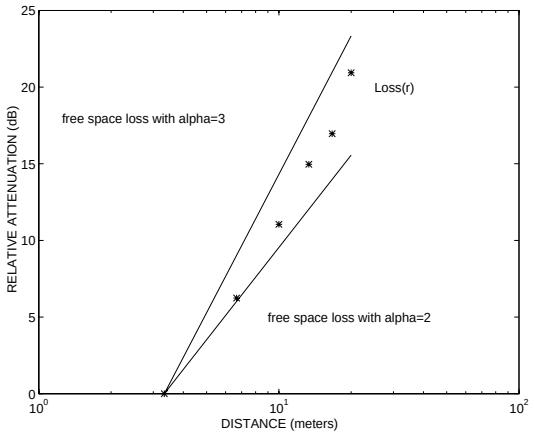

Fig. 3. Power attenuation $L(r)$ at distance r from the transmitter.

range (m)	forest depth (m)	Theo. Loss (dB)	Est. Peak (dB)
3	0	0	0
6.1	3	1.5	0.4
9.1	6.1	3	2.8
12.2	9.1	4.4	4.9
15.2	122	5.9	7.9
18.3	15.2	7.1	8.8

TABLE II
THEORETICAL AND ESTIMATED VALUES OF FORESTATION LOSSES AS A FUNCTION OF RANGE.

where L_f is the forestation loss in dB, f is the frequency in GHz and d_f is the depth into the forest in meters.

Table II shows the theoretical value of the forestation loss at $f = 1.2GHz$ determined using the narrowband model, as well as the experimental peak estimated loss calculated at at $f = 1.2GHz$ using the spectrum of the received signal $x(t)$. The values show that the narrowband model can be applied to the UWB case.

IV. MULTIPATH CHANNEL CHARACTERIZATION

Degradation due to multipath channel can be separated from the effect of imperfect reconstruction of the received waveform by considering the infinite RAKE (IRAKE) receiver. IRAKE receiver is RAKE receiver with unlimited resources (correlators) so that it would, in principle, construct a filter matched to the received waveform perfectly. This serves as the best case (bench mark) for RAKE receiver design. Multipath degradation is characterized by computing the IRAKE receiver correlator output, $R_{\mathrm{IRAKE}}(\zeta)$ and compare it with the correlation function of an ideal channel,$R_{\mathrm{Ideal}}(\zeta)$ (in the absence of multipath). $R_{\mathrm{IRAKE}}(\zeta)$ is computed for different locations from the measured responses. Figure 4 shows $R_{\mathrm{IRAKE}}(\zeta)$ function calculated for different measurements and figure 5 illustrates a typical ensemble of this functions that must be considered developing a modulation technique based on pulse position modulation [Ramirez, 1997]. This suggest that multipath places fundamental limits on the ability to extend pulse-position modulation techniques to M-ary case.

V. CONCLUSIONS

A pilot experiment of UWB propagation measurements has been made in rural terrain using a periodic pulse generator that transmits pulses with bandwidth on the order of 1.3 GHz at every 500 nanoseconds. Multipath measurements are made. The same absolute delay reference for all recorded multipath profiles is achieved, and the time delay measurements of the signals arriving to the received antenna via different propagation paths are made. Mean delay, delay spread, propagation loss and forestation losses are calculated. A new concept called Infinite RAKE Receiver is introduced, which serves as the best case (bench mark) for RAKE receiver design and permits to estimate the degradation due to multipath channel. This pilot experiment serves as a preliminary look at the UWB channel for rural terrain but more extensive measurements are necessary in the future for complete statistical characterization of such channel.

Acknowledgments

The authors wish to thank Troy Fuqua, Glenn Wolenec and Larry Fullerton of Time Domain Systems, and Paul Withington of Pulson Communications for several helpful discussions concerning the technology, capabilities, and signal processing of impulse signals.

References

[Hashemi, 1993] H. Hashemi. *"The Indoor Propagation Channel,"* Proc. IEEE Vol. 81, issue 7, July 1993, pp. 943-968.

[Ramirez, 1997] F. Ramírez-Mireles, M. Z. Win and R. A. Scholtz, *"Signal Selection for the Indoor Wireless Impulse Radio Channel,"* IEEE VTC'97 Proceedings, May 1997.

[Saleh, 1987] A. M. Saleh and R A. Valenzuela, *"A Statistical Model for the Indoor Multipath Propagation,"* IEEE JSAC Vol. SAC-5, No. 2, February 1987, pp. 128-137.

[Weissoerger, 1982] M. Weissoerger, *"An Initial Critical Summary of Models for Predicting the Attenuation of Radio Waves by Trees,"* IIT Research Institute, July 1982.

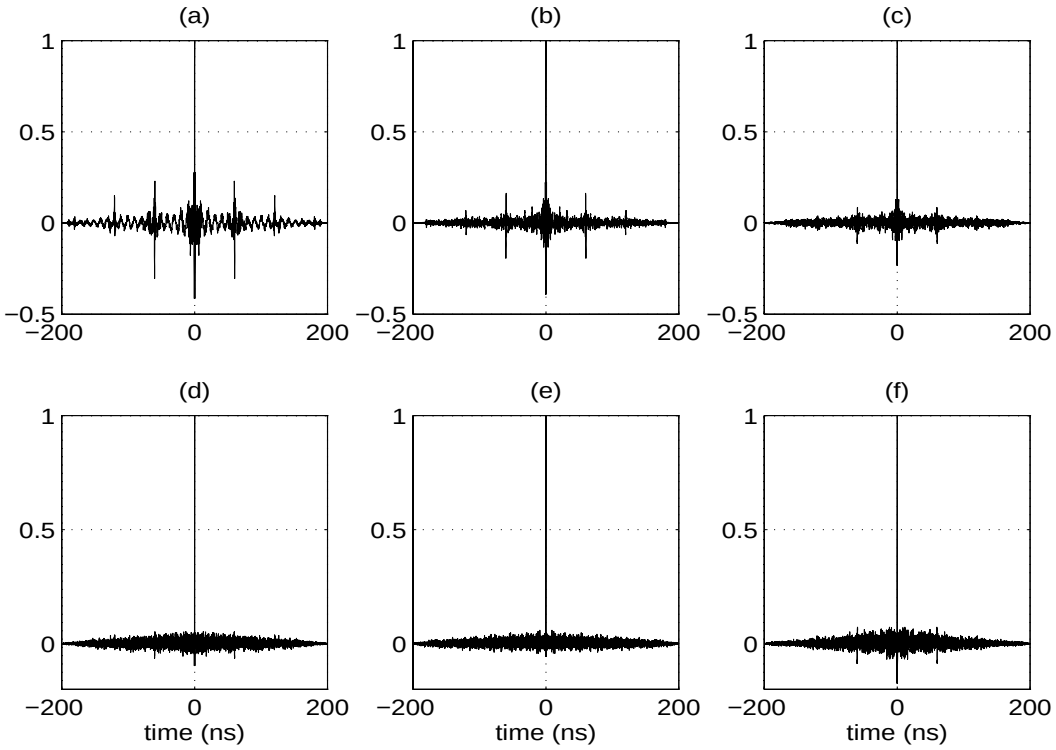

Fig. 4. $R_{\mathrm{IRAKE}}(\zeta)$ calculated from signal received at distance c feet from the transmitter and d feet depth into the line of foliage. (a) c=10, d=0. (b) c=20, d=10. (c) c=30, d=20. (d) c=40, d=30. (e) c=50, d=40. (f) c=60, d=50.

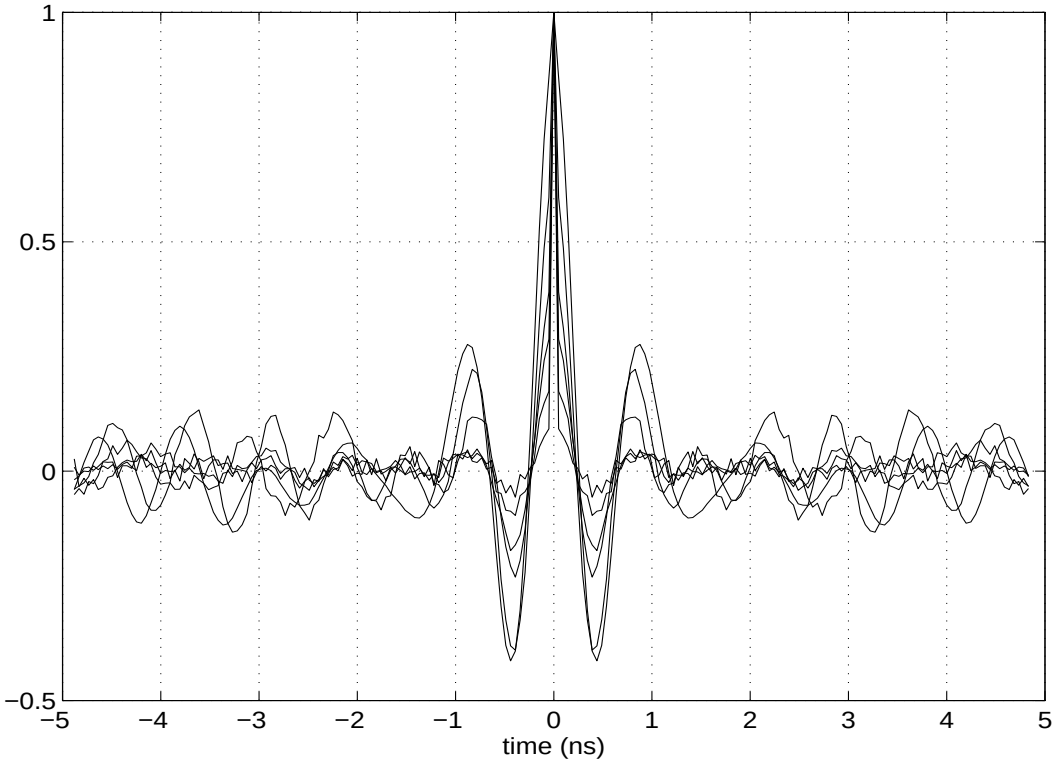

Fig. 5. $R_{\mathrm{IRAKE}}(\zeta)$ in figure 4 is shown here superimposed.